Supporting Information

for

Efficient Activation of Peracetic Acid via a Defect-Rich Carbon Nanotubes@Co_3O_4 Three-Dimensional Network for Antibiotics Removal: Mechanism Insights and Practical Water Remediation

Jianqing Wu[a], Yingfei Wang[b,c], Zongshun Yu[a], Dandan Wei[a], Daguang Li[a], Chenghui Wen[a], Ping Chen[a], Haijin Liu[d], Wenying Lv[a], Guoguang Liu[a]*

[a]Guangdong Key Laboratory of Environmental Catalysis and Health Risk Control, Guangdong-Hong Kong-Macao Joint Laboratory for Contaminants Exposure and Health, School of Environmental Science and Engineering, Guangdong University of Technology, Guangzhou 510006, China

[b]School of Social and Ecological Civilization Teaching & Research, Party School of Guangdong Provincial Committee of C.P.C. (Chinese Academy of Governance)

[c]School of Environmental Science and Engineering, Guangdong Provincial Key Laboratory of Environmental Pollution Control and Remediation Technology, Sun Yat-sen University, Guangzhou, 510006, China

[d]School of Environment, Henan Normal University, Key Laboratory for Yellow River and Huaihe River Water Environment and Pollution Control, Xinxiang 453007, China

* **Corresponding Author**: Guoguang Liu

E-mail: liugg615@163.com

Telephone: +86-20-39322547
Fax: +86-20-39322548

Text S1. Chemicals

Commercial peracetic acid was purchased from Damao Reagent Factory (Tianjin, China), sulfonamides (SAs), Cobalt nitrate hexahydrate, 2-Methylimidazole (2-MeIM), carbon nanotubes (CNTs), humic acid (HA), 5,5-dimethyl-1-pyrroline N-oxide (DMPO), 2,2,6,6-tetramethyl-4-piperidinol (TMP), Hydrogen peroxide (H_2O_2, 30% w/w), tert-butanol (TBA) and acetic acid were provided by Aladdin Co., Ltd. (Shanghai, China). All other chemicals and reagents were provided by Sinopharm Chemical Reagent Co., Ltd. (Shanghai, China). All reagent solutions were prepared using deionized (DI) water from a Millipore Milli-Q Ultrapure Gradient A10 purification system.

Text S2. Determination of concentration of SDZ.

High-performance liquid chromatography (HPLC-20A, Shimadzu, Japan) system was used to measure the concentrations of SMZ. The system constituted of two Shimadzu LC-20AD pumps (Shimadzu, Japan) and a Shimadzu SPD-M20A photodiode array detector was equipped with a Zorbax Eclipse XDB-C18 (4.6 x 150 mm, 5μm). The chromatographic column conditions of SDZ were as follow: mobile phase: methanol/ formic acid buffer solution (30:70 v/v containing 0.2 % formic acid); flow rates: 1 mL/min; injection volume: 20μL; temperature: 35°C; detection wavelength: 262 nm.

Text S3. Identification of catalytic by-products of SDZ.

The intermediates of SDZ in the process of catalytic degradation were identified by high-resolution liquid chromatography (Thermo Scientific Ultimate 3000 RSLC) and HRAM LC-MS/MS (Q Exactive Orbitrap). When the column temperature was 40 ℃, a Hypersil GOLD C18 (100 x 2.1 mm, 1.9 μm) was applied to separate the by-products. The solution containing 0.1 % (v/v) formic acid as eluent A, and methanol as eluent B was used for elution at a flow rate of 0.3 mL/min. Both of the positive and negative modes were used to proceed Mass spectral analysis.

Text S4. Characterizations of samples

The crystal phases and structures of the samples were measured using X-ray powder diffraction (XRD, UItima IV, and RIGAKU). The morphologies and microstructures were measured by scanning electron microscopy (SEM, Hitachi, SU8010) and transmission electron microscopy (TEM, FEI, TALOS 200X). X-ray photoelectron spectroscopy (XPS) was performed using a Thermo Scientific K-Alpha Nexsa instrument. N_2 adsorption-desorption experiments were used to determine the Brunauer-Emmett-Teller (BET) surface area using a physisorption analyzer (ASAP 2460, Micromeritics).

Text S5. Quantitative analysis of chemical PMSO and $PMSO_2$

Further, the identification of ^{18}O isotope labeling of $PMSO_2$ and degradation intermediates of organic substrates were identified using liquid chromatography combined with hybrid quadrupole time-of-flight mass spectrometry. UPLC system equipped with an electron spray ionization source was used to quantity the PMSO and $PMSO_2$. The oxidation of PMSO in the d-CNTs@Co_3O_4-NS/PAA system was used to detect the generation of high-valent Co species. The chromatographic separation was carried out on a Waters C18 column (4.6×50 mm, 1.7 μm particle size) using acetonitrile and deionized water containing 0.1% formic acid as the mobile phase with a volume ratio of 10/90 at a flow rate of 0.1 mL/min. An isocratic elution method of acetonitrile/H_2O (containing 0.1% formic acid) (v: v=10: 90) was carried out for 5min. An electrospray ionization source in the positive ionization mode was used for LCMS analysis with the mass calibration. The ^{18}O isotope-labeling experiments were performed in 5.0 mL of $H_2{}^{18}O$. A UPLC identified the $^{16}O/^{18}O$ isotope-labeled $PMSO_2$ in a positive mode. Methyl alcohol (eluent A) and 0.1% formic acid in water (eluent B) with a volume ratio of A: B=20: 80 at a flow rate of 0.4 mL•min^{-1} was equipped as the isocratic elution mobile phase.

Text S6. The identification of reactive species with electron paramagnetic resonance

The determination of reactive species were performed using the electron paramagnetic resonance (EPR) with BRUKER model A300 measurements technique. EPR technique was utilized for the estimation of reactive species with 5,5-dimethyl-1-pyrroline-N-oxide (DMPO) for the identification of organic radicals (R-O•) and hydroxyl radicals (•OH), and 2,2,6,6-tetramethyl-4-piperidinol (TMP) for $^1O_2$ using BRUKER model A300 measurements.

Text S7. Electrochemical measurements

The electrochemical properties of the photocatalysts were examined via a CHI-760e electrochemical workstation using a Pt wire electrode and saturated calomel electrodes (SCE) as the counter electrode and reference electrode, respectively. A 0.1 M Na_2SO_4 aqueous solution was used as the electrolyte (pH=5.6). The sample suspensions were mixed with Nafion 117 and then drop-coating on ITO glass (1 cm×1 cm) to prepare a working electrode. In the current response curve (i-t) measurement experiment and measurement of the open-circuit voltage, a suitable bias voltage near the open-circuit voltage was first measured.

Table S1 Isothermal N_2 adsorption–desorption of different samples

Samples	BET surface areas (m^2/g)	Average pore size (nm)	Total pore volume (cm^3/g)
d-CNTs@Co_3O_4-NS	55.09	32.51	0.4752
CNTs@Co_3O_4	44.52	12.56	0.1531

Table S2. Intermediate compounds identified by HPLC/MS/MS during the catalytic degradation of SDZ

compound	Rt/min	m/z	Molecular formula	Probable structure
SDZ	13.78	250	$C_{10}H_{10}N_4O_2S$	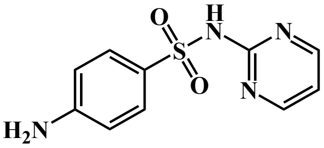
P-95	12.75	95	$C_4H_5N_3$	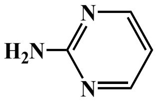
P-111	1.00	111	$C_4H_5N_3O$	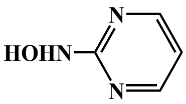
P-172	5.64	172	$C_6H_8N_2O_2S$	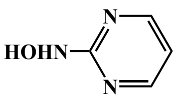
P-266	10.47	266	$C_{10}H_{10}N_4O_3S$	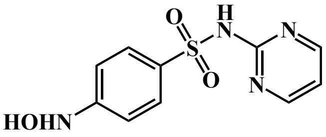
P-264	10.39	264	$C_{10}H_8N_4O_3S$	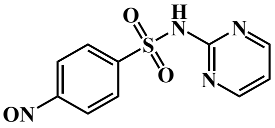
P-280	9.80	280	$C_{10}H_8N_4O_4S$	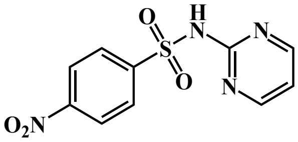
P-214	12.97	214	$C_7H_{10}N_4O_2S$	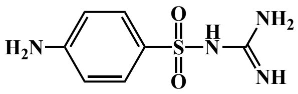
P-274	15.98	274	$C_7H_6N_4O_6S$	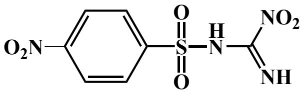
P-186	0.85	186	$C_{10}H_{10}N_4$	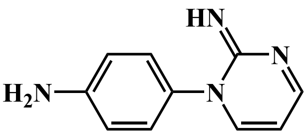

P-202	0.93	202	$C_{10}H_{10}N_4O$	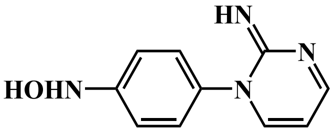
P-216	1.00	216	$C_{10}H_8N_4O_2$	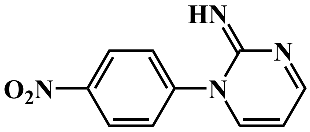

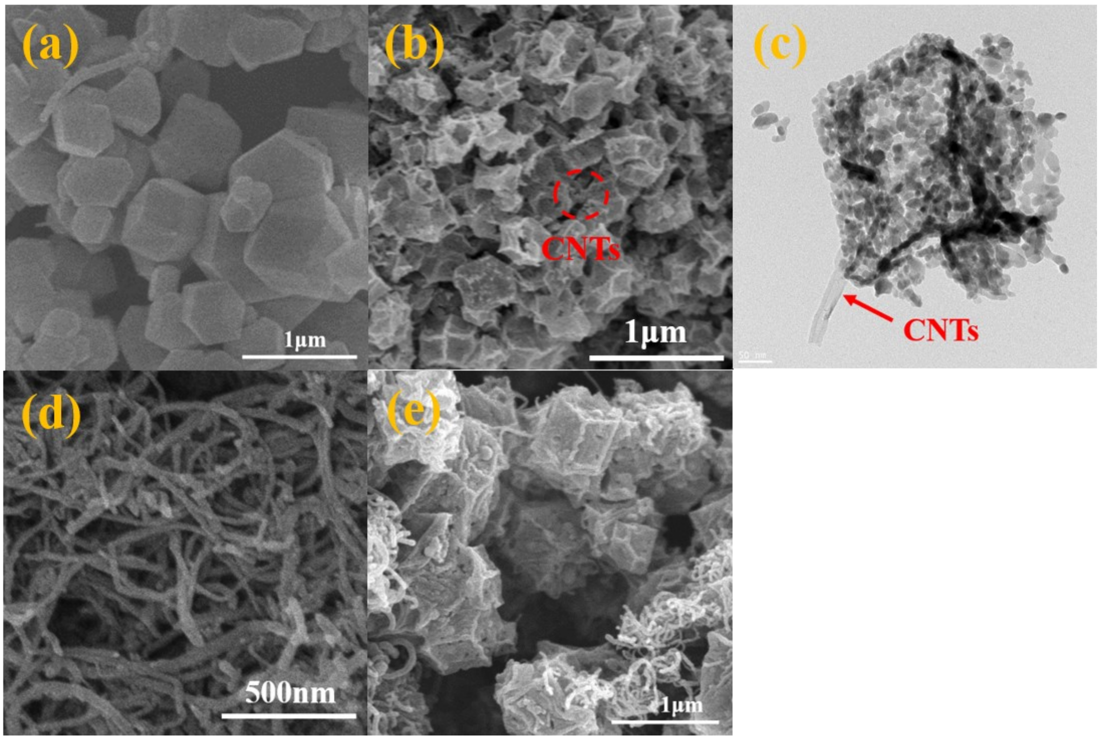

Figure S1. (a) SEM images of CNTs@ZIF-67; (b) SEM images of CNTs@Co_3O_4; (c) TEM images of CNTs@Co_3O_4; and SEM image of (d) d-CNTs; (e) d-CNTs@Co.

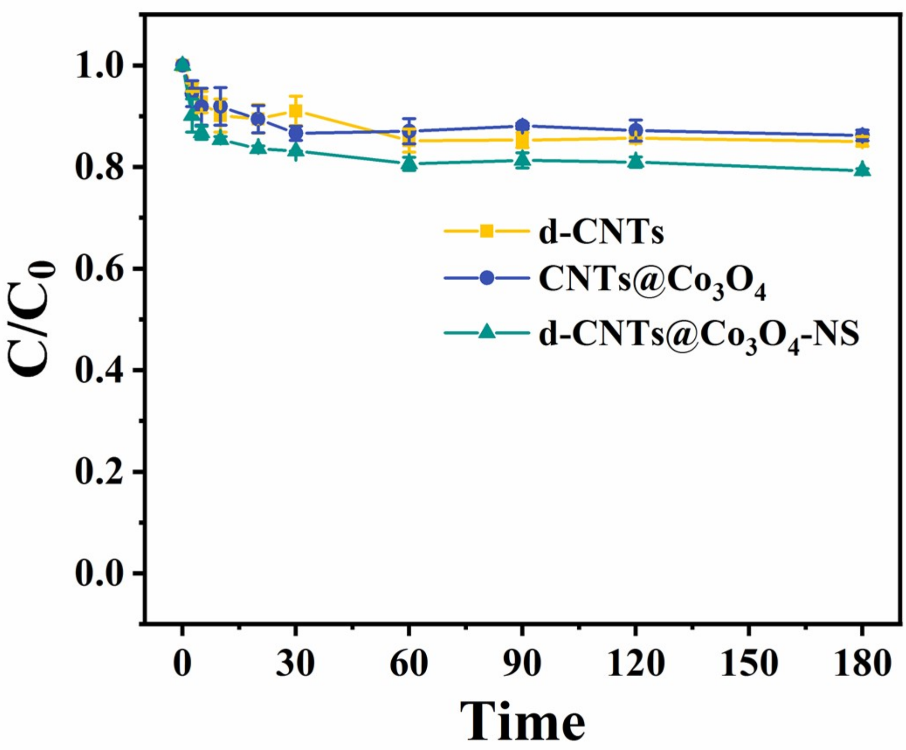

Figure S2. The adsorption effect of SDZ with different samples in 180 min.

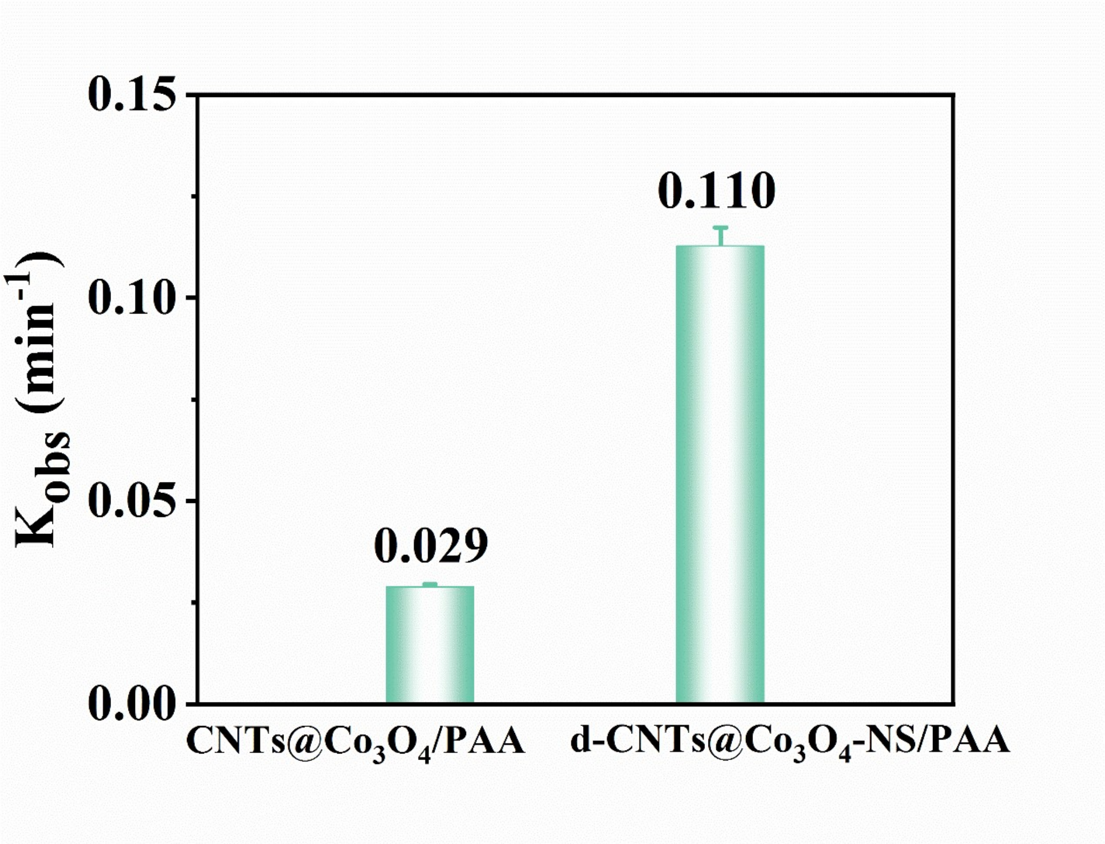

Figure S3. Degradation kinetic rate constant of CNTs@Co_3O_4/PAA and d-CNTs@Co_3O_4-NS/PAA systems. Conditions: [SDZ] = 8 mg/L, [PAA] = 0.5 mM, [samples] = 0.1 g/L temperature 23 ± 2 °C.

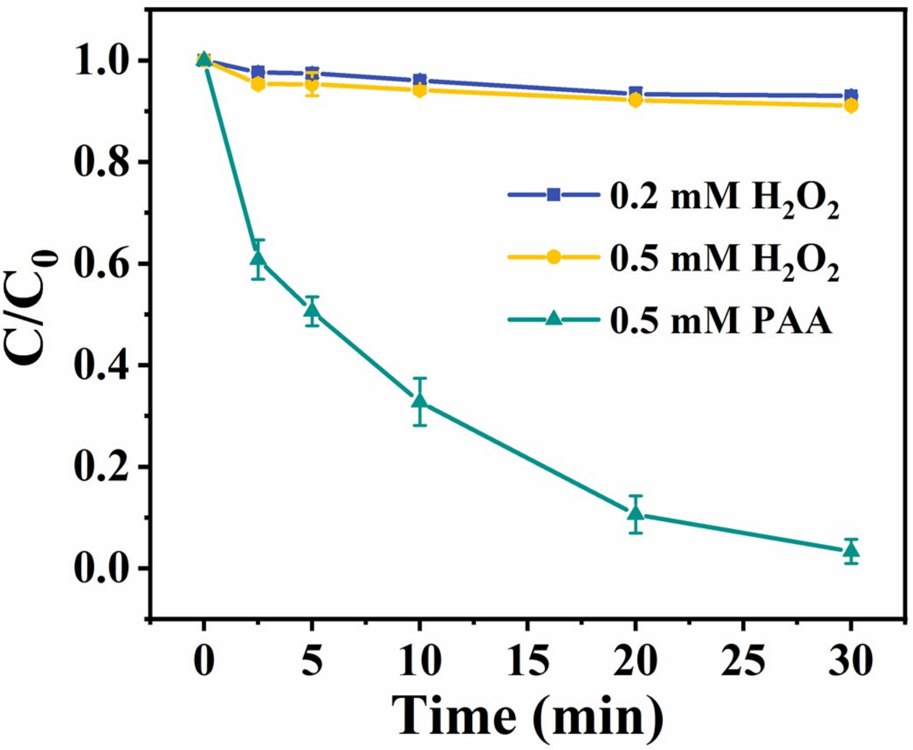

Figure S4. Degradation kinetic rate constant of d-CNTs@Co_3O_4-NS/PAA and d-CNTs@Co_3O_4-NS/H_2O_2 systems. Conditions: [SDZ] = 8 mg/L, [samples] = 0.1 g/L temperature 23 ± 2 °C.

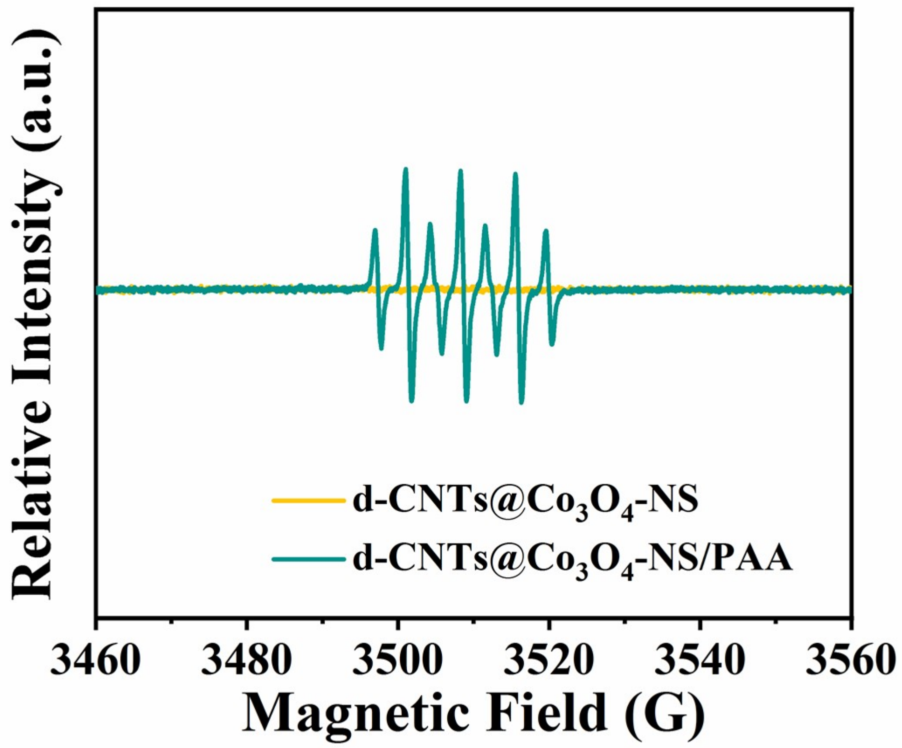

Figure S5. EPR spectra of DMPOX. Conditions: [DMPO] = 50 mM, [PAA] = 0.5 mM, [d-CNTs@Co$_3$O$_4$-NS] = 0.1 g/L, reaction time 5 min.

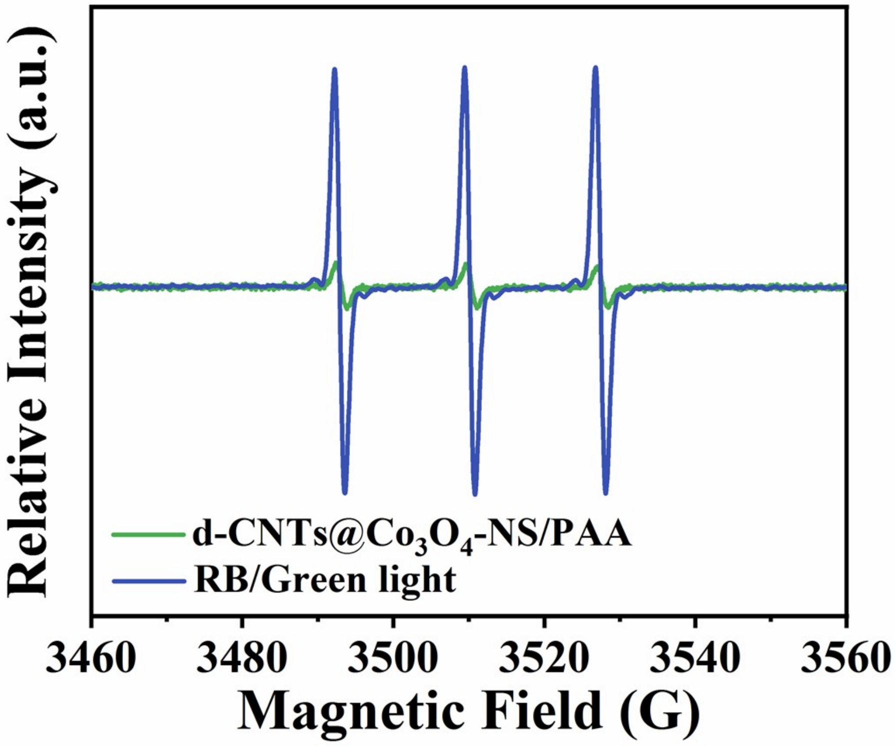

Figure S6. EPR spectra of TMP-$^1O_2$ adduct. Conditions: [TMP] = 50 mM, [PAA] = 0.5 mM, [RB] = 0.2mM, [d-CNTs@Co_3O_4-NS] = 0.1 g/L, reaction time 5 min.

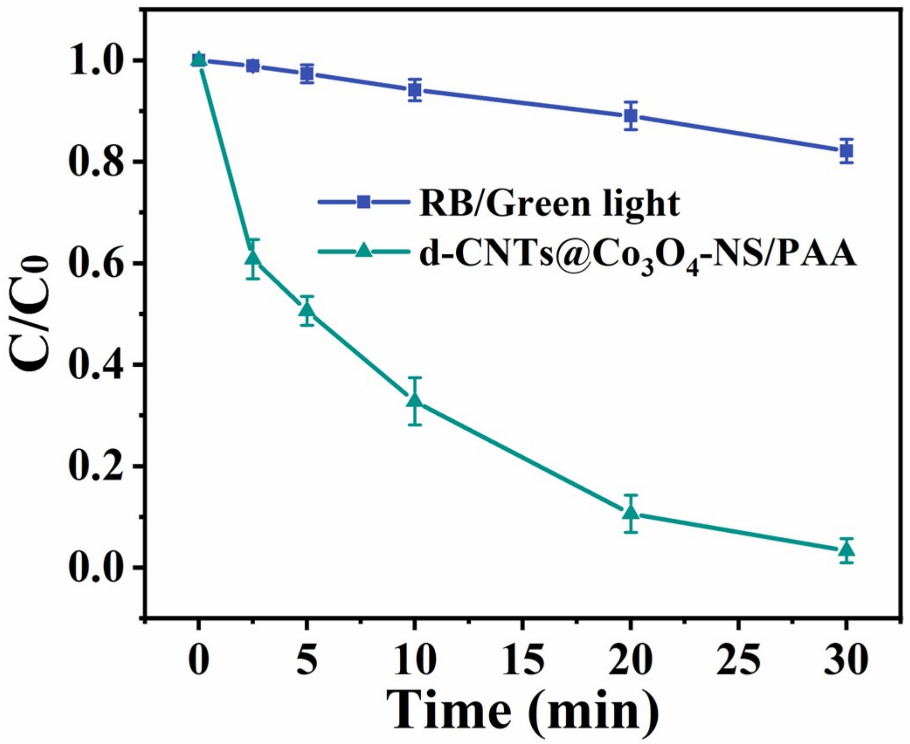

Figure S7. Degradation of SDZ with RB/green light system. Conditions: [SDZ] = 8 mg/L, [PAA] = 0.5 mM, [RB] = 0.2mM, [d-CNTs@Co_3O_4-NS] = 0.1 g/L.

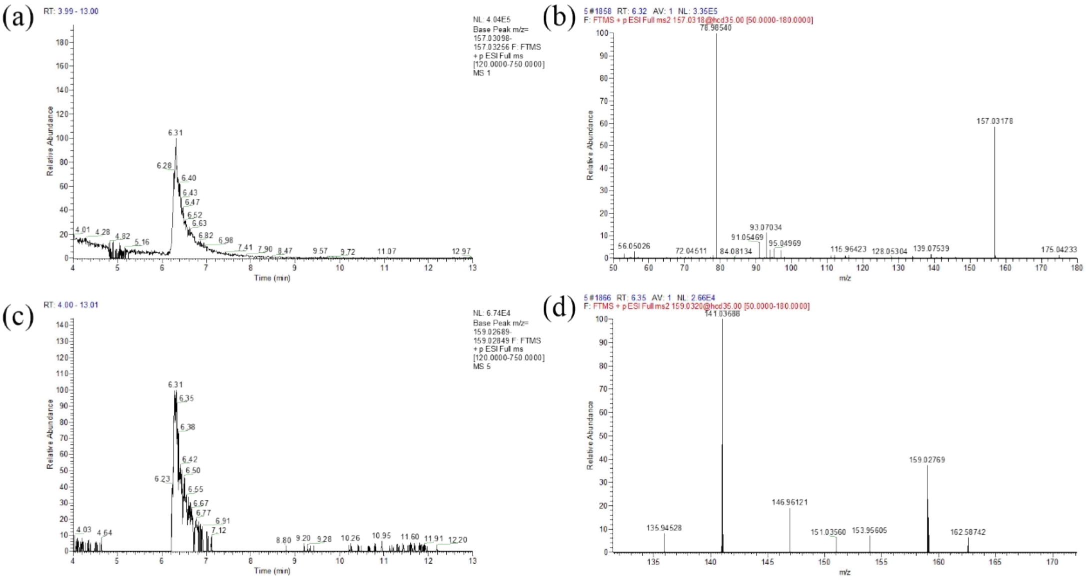

Figure S8. Chromatogram and mass spectral analyses of the PMS^{16}O^{16}O and PMS^{18}O^{16}O.

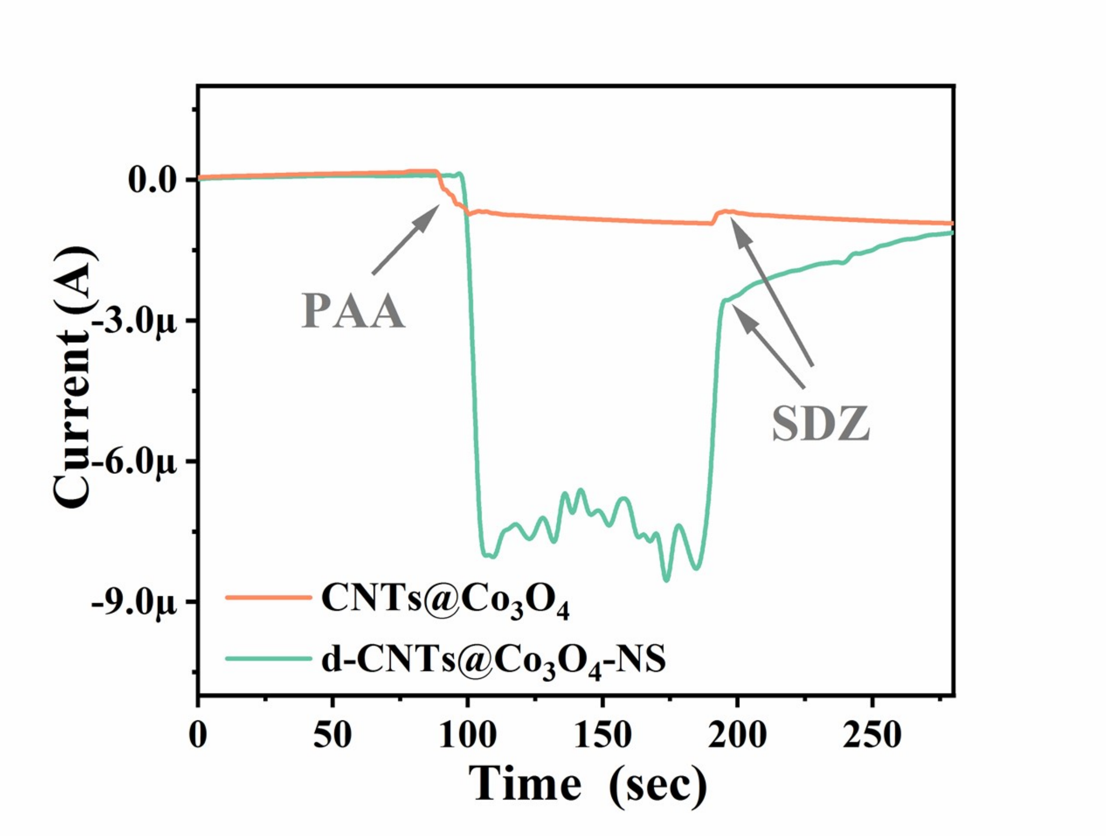

Figure S9. Amperometric i-t curve measurements upon the addition of PAA and SDZ using d-CNTs@Co_3O_4-NS and CNTs@Co_3O_4 as the working electrode.

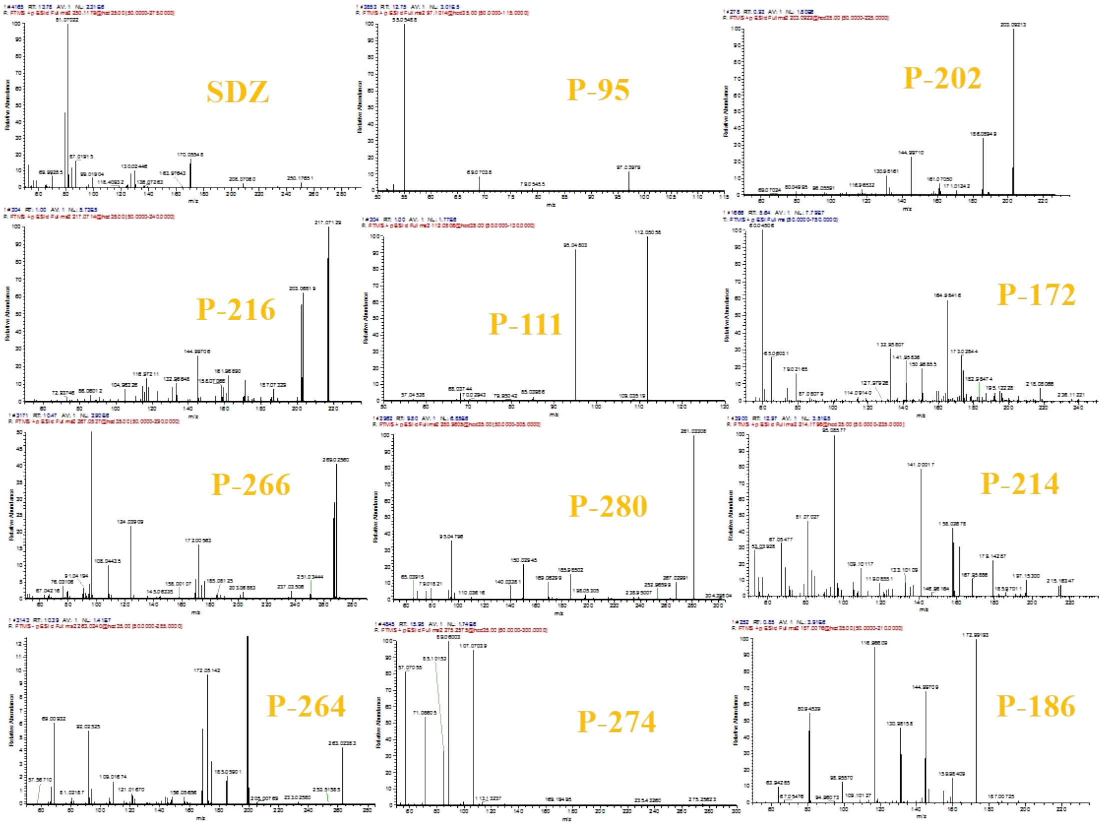

Figure S10. MS/MS fragmentation analyses of the observed transformation products of SDZ.

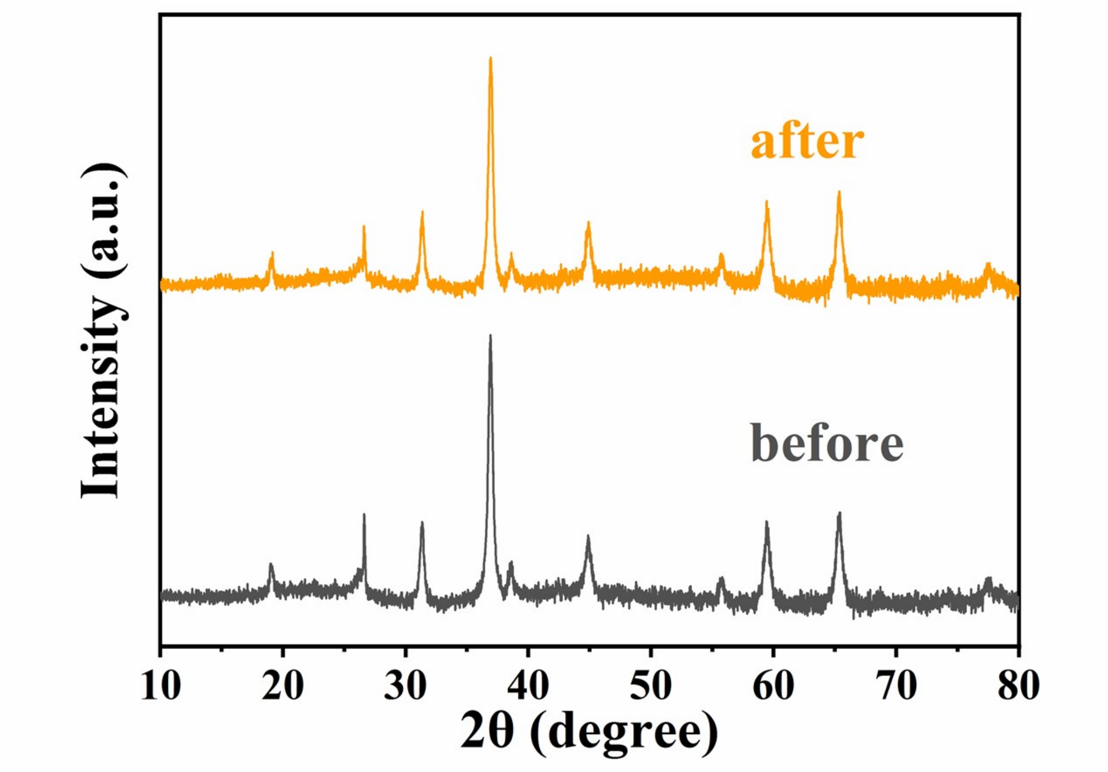

Figure S11. XRD spectrum of d-CNTs@Co_3O_4-NS before and after reaction.

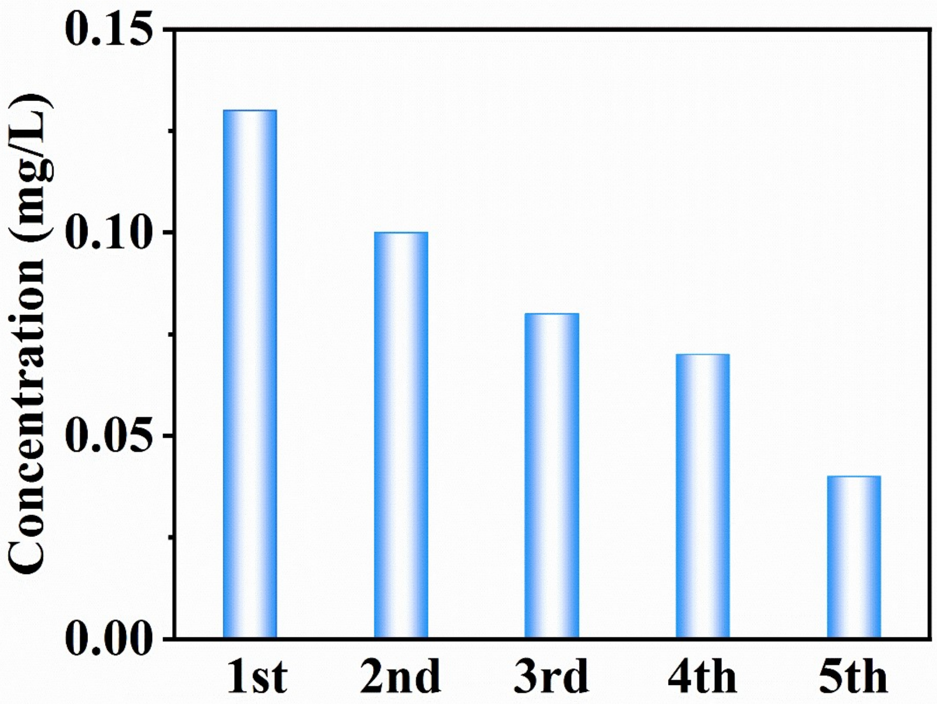

Figure S12. The leaching Co ions concentration after five times reaction.